# Flux driven transport modelling of ASDEX Upgrade discharges with the quasilinear gyrokinetic code QuaLiKiz

O. Linder[1,2], J. Citrin[1], G.M.D. Hogeweij[1], C. Angioni[3], C. Bourdelle[4], F.J. Casson[5], A. Ho[1], F. Koechl[6], M. Sertoli[3], the EUROfusion MST1 Team* and the ASDEX Upgrade Team

[1]*DIFFER - Dutch Institute for Fundamental Energy Research, 5612 AJ Eindhoven, the Netherlands,* [2]*Eindhoven University of Technology, 5612 AJ Eindhoven, the Netherlands,* [3]*Max-Planck-Institut für Plasmaphysik, Boltzmannstraße 2, D-85748 Garching, Germany,* [4]*CEA, IRFM, F-13108 Saint-Paul-lez-Durance, France,* [5]*CCFE, Culham Science Centre, Abingdon, Oxon, OX14 3DB, UK,* [6]*ÖAW/ATI, Atominstitut, TU Wien, 1020 Vienna, Austria,*
**See author list of Meyer et al. "Overview of progress in European Medium Sized Tokamaks towards an integrated plasma-edge/wall solution", accepted for publication in Nucl. Fusion*

In a commercial fusion reactor, plasma facing components made of tungsten (W) are envisaged due to the material's low fuel retention and low erosion under high heat and particle fluxes [1,2]. Yet, strong line radiation of non-fully ionized tungsten at fusion relevant temperatures [3] can strongly cool the central plasma, deteriorating fusion performance. Consequently, central W-accumulation has to be avoided to keep concentrations in the core plasma below $\sim 10^{-4}$ [4]. In ASDEX Upgrade (AUG), central wave heating has been applied regularly for W-impurity density control [5–7]. Yet, complete understanding of all W-transport mechanisms involved is still an outstanding issue. In present day devices, heavy impurity transport is dominated by neoclassical transport inside half radius [6–9]. Additionally, outward W-transport is occasionally facilitated both directly and indirectly by saturated $(m,n) = (1,1)$ MHD modes [10, 11], affecting background profiles and thus neoclassical transport. The same holds for transport enhancement by central wave heating [6, 11]. Since dominating neoclassical W-impurity transport depends i.a. strongly on the main ion density and temperature profiles [8,9], accurate modelling of main ion transport is a vital prerequisite to ultimately simulate trace W-impurity transport.

Towards this goal, the fast quasilinear gyrokinetic code QuaLiKiz [12, 13] is coupled to the transport code JETTO [14, 15] and used for the first time for integrated modelling of an AUG discharge. QuaLiKiz calculates turbulent heat, particle and momentum fluxes driven by ITG, TEM and ETG modes. The computed quasilinear fluxes have been validated against nonlinear simulations [12] and tested for predicting temperatures, densities and toroidal velcities in H mode pulses [13, 16]. Thanks to recent numerical improvements [13], QuaLiKiz can now be used routinely for time evolving predictions, modelling 1 s of plasma evolution in $\sim$ 100 CPUh. In this study, predictive heat and particle simulations in the presence of light impurities are performed in the plasma core to validate the main ion transport mechanisms calculated against experimentally obtained temperature and density profiles for AUG discharge #31115.

The discharge analysed (cf. Fig. 1) is dominantly heated by NBI ($B_{\mathrm{tor}} = 2.48\,\mathrm{T}$, $I_{\mathrm{p}} = 1.00\,\mathrm{MA}$, $q_{95} = 3.96$). Additional on-axis ECRH of 1.35 MW is applied during the entire discharge. At $t = 3.5\,\mathrm{s}$, a fourth NBI source is coupled to the plasma, increasing total NBI power from 7.34 MW to 9.67 MW. Simultaneously, a transition in MHD activity from sawteeth to a continuous $(m,n) = (1,1)$ mode is observed by on-axis ECE. As a result, W-impurities are flushed out of the center, creating a deeply hollow W-density profile (cf. Fig. 1(d)). Since the plasma parameters differ vastly in phases of different NBI power, simulations are performed in the intervals $t_1 \in [2.5\,\mathrm{s}, 3.5\,\mathrm{s}]$ and $t_2 \in [5.0\,\mathrm{s}, 6.0\,\mathrm{s}]$, corresponding to 17.2 and 18.6 energy confinement times $\tau_{\mathrm{E}}$ respectively. Averaged plasma profiles are constructed from raw data using Gaussian process regression (see Fig. 2), whereas particle deposition and power profiles are obtained from the TRANSP code. Anomalous fluxes are calculated by QuaLiKiz in the turbulence dominated region $\rho_{\mathrm{tor}} \in [0.20, 0.85]$, treating the plasma profiles for $\rho_{\mathrm{tor}} > 0.85$ as boundary conditions. Core MHD activity is mimicked by including additional transport coefficients, derived from heat and particle balance equations of the averaged plasma profiles.

Heat and particle transport are predicted satisfactorily inside the boundary condition (see Fig. 2). Calculated plasma profiles agree within 10 % with the absolute values of the experimental average. In terms of the standard deviation $\sigma$ of the regression results, agreement is often within $1\,\sigma$, usually within $2\,\sigma$. Particle transport is particularly well captured near the pedestal. Around mid-radius, excellent agreement is achieved for time slice $t_1$. Although transport is slightly underestimated in the high NBI-power case, central density profiles still agree within 10 %. Good agreement in heat transport calculations is observed in the same region, while be-

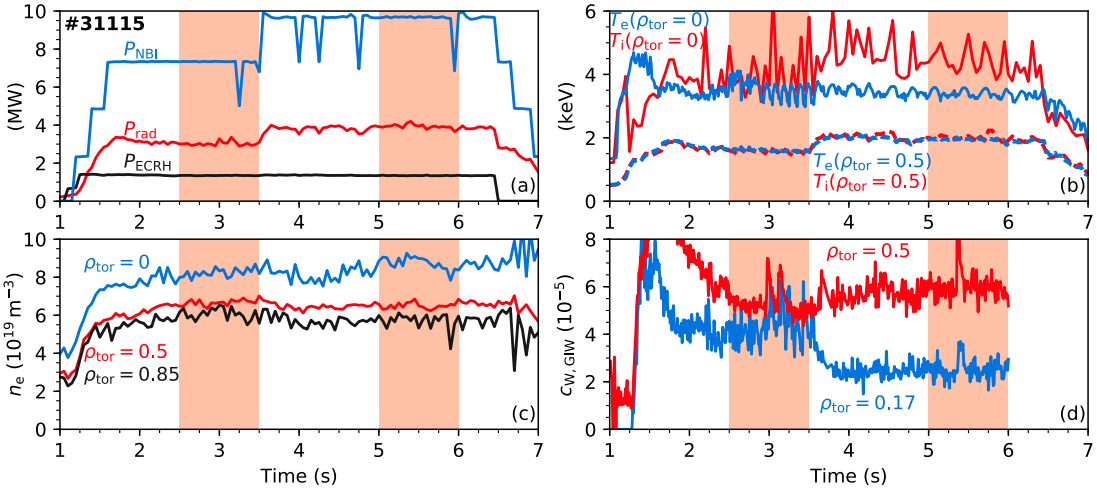


Fig. 1: Time traces of (a) the NBI, ECRH and radiated powers, (b) the species temperatures $T_{\mathrm{s}}$ on axis and at mid-radius, (c) the electron density $n_{\mathrm{e}}$ on axis, at mid-radius and on top of the pedestal, and (d) the W-concentration $c_{\mathrm{W,GIW}}$ from X-ray spectroscopy (GIW) at $\rho_{\mathrm{tor}} = 0.17$ and mid radius for AUG discharge #31115. Shaded regions indicate the time slices used for predictive heat and particle simulations.

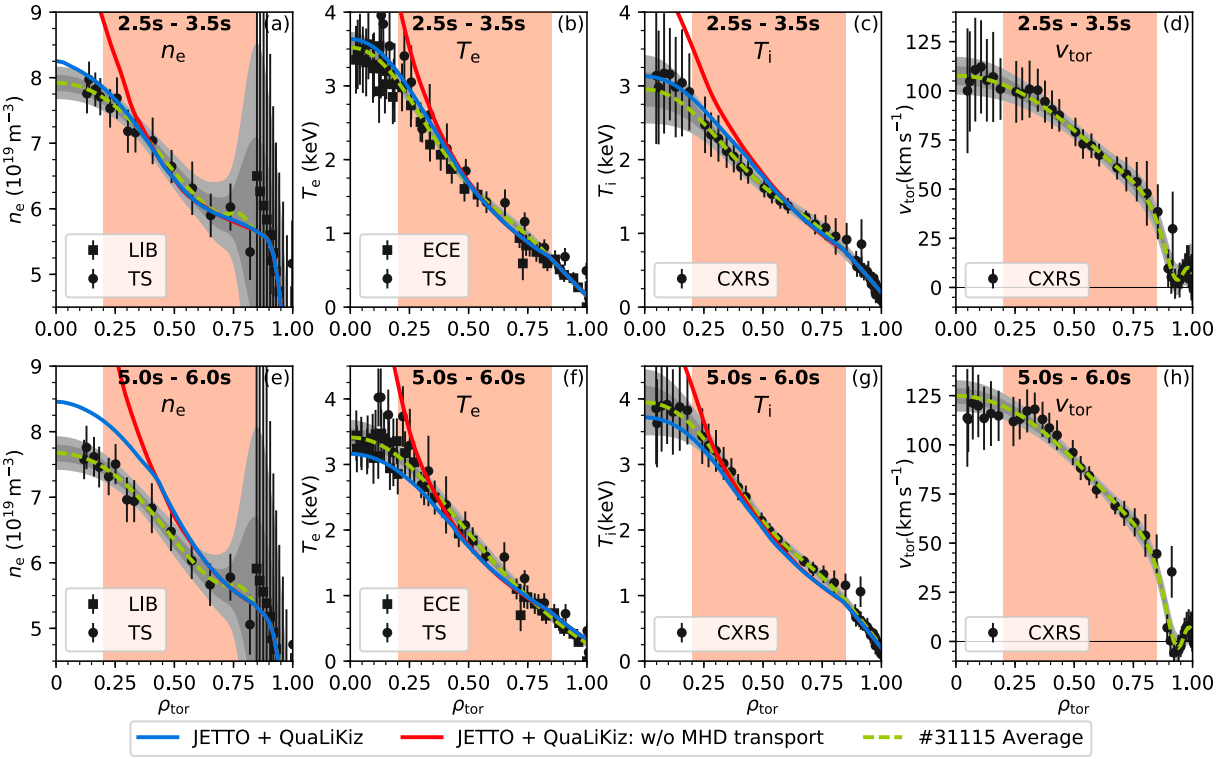


Fig. 2: Predictive particle and heat simulations performed by JETTO and QuaLiKiz, with additional transport due to MHD effects included (solid blue) or omitted (solid red), compared to the averaged plasma profiles (dashed green) with confidence intervals of $1\,\sigma$ and $2\,\sigma$ (grey) for both time slices. (a,e) Averaged $n_e$-profiles were obtained from lithium beam emission spectroscopy (LIB) and Thomson scattering spectroscopy (TS), (b,f) averaged $T_e$-profiles from electron cyclotron emission (ECE) and TS, and averaged (c,g) $T_i$- and (d,h) $v_{tor}$-profiles from charge exchange recombination spectroscopy (CXRS).

ing slightly overestimated close to the boundary condition. This effect is particularly prominent in the high NBI-power case. Although excellent agreement is obtained between predicted and experimental temperature gradients $\nabla_{\rho_{tor}} T_s$ for $\rho_{tor} \lesssim 0.6$, calculated temperature profiles are effectively shifted to lower temperatures due to pedestal transport overprediction.

Agreement in particle and heat transport inside the $q = 1$ surface is obtained only when prescribing enhanced transport coefficients to mimic MHD activity. Neglecting the influence, plasma profiles are severely overestimated (cf. Fig. 2), thus highlighting the significance of MHD driven central core transport. Since the corresponding transport coefficients were calculated from heat and particle balances, transport is usually predicted exactly for $\rho_{tor} \lesssim 0.30$ as MHD contributions dominate in this region. The additional ion heat diffusivity due to MHD activity is found to be $\chi_i \sim 1.3\,\mathrm{m^2\,s^{-1}}$ for both phases. On axis, electron heat transport coefficients are similarly $\chi_e \sim 15\,\mathrm{m^2\,s^{-1}}$, but are generally more prominent off-axis in the high NBI-power case. As MHD driven particle transport is increased in the presence of the continuous $(1,1)$ mode ($D_{eff}(t_2) \sim 0.40\,\mathrm{m^2\,s^{-1}}$, $D_{eff}(t_1) \sim 0.25\,\mathrm{m^2\,s^{-1}}$), this particular MHD activity is suspected to greatly facilitate outward W-transport, creating the deeply hollow W-density profile observed.

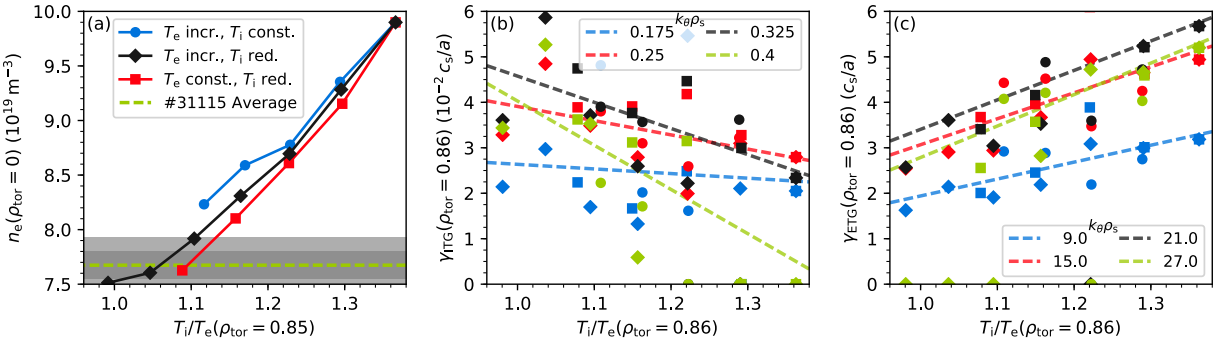


Fig. 3: Plasma response to the $T_i/T_e|_{bc}$ boundary condition for the time slice $t_2 \in [5.0\,s, 6.0\,s]$. From the temperature profiles obtained by Gaussian process regression ($T_i/T_e|_{ped} = 1.37$), different ratios $T_i/T_e$ are obtained by increasing $T_e$ (circles), reducing $T_i$ (squares), or symmetrically increasing $T_e$ and reducing $T_i$ (diamonds) at the pedestal. (a) Predicted on-axis electron density compared to the averaged plasma profile (dashed green) with confidence intervals of $1\,\sigma$ and $2\,\sigma$ (grey). (b) Growth rates of ITG turbulence at the pedestal for different wavenumbers $k_\theta\rho_s$. (c) Growth rates of ETG modes for different $k_\theta\rho_s$.

The simulations are found to be sensitive to the imposed ion to electron temperature $T_i/T_e|_{bc}$ boundary condition at $\rho_{tor} = 0.85$. For $T_i/T_e|_{bc} > 1.2$, severe density peaking is observed (cf. Fig. 3(a)), whereas heat transport is less affected by the choice of $T_i/T_e|_{bc}$. Under these conditions, ITG modes are stabilized (cf. Fig. 3(b)), significantly reducing ion heat and particle transport. Simultaneously, electron heat transport is increased as ETG turbulence is destabilized (cf. Fig. 3(c)). Due to ion-electron heat exchange, overall heat transport is only slightly affected by changing the $T_i/T_e$ boundary conditions. As ETG turbulence does not drive particle transport, the reduced ITG drive cannot be countered. Thus overall particle transport is reduced significantly, yielding strongly peaked density profiles. As a result, careful analysis of raw data using Gaussian process regression was carried out to constrain $T_i/T_e|_{bc}$ within reasonable bounds.

In this study, the main ion transport in an AUG discharge has been simulated successfully by QuaLiKiz under the influence of a continuous $(1,1)$ MHD mode, thus paving the way for trace W-simulations in the same discharge with QuaLiKiz and neoclassical transport to reproduce the central W-density behavior observed as shown in previous, non-integrated modelling [9–11].

**Acknowledgements:** This work has been carried out within the framework of the EUROfusion Consortium and has received funding from the Euratom research and training programme 2014-2018 under grant agreement No 633053. The views and opinions expressed herein do not necessarily reflect those of the European Commission.

[1] H. Bolt *et al*. J. Nucl. Mater. **329-333**, 66 (2004).
[2] R.A. Causey. J. Nucl. Mater. **300**, 91 (2002).
[3] D.E. Post and R.V. Jensen. At. Data Nucl. Data Tables **20**, 397 (1977).
[4] R. Neu *et al*. J. Nucl. Mater. **241-243**, 678 (1997).
[5] R. Neu *et al*. Plasma Phys. Control. Fusion **44**, 811 (2002).
[6] R. Dux *et al*. J. Nucl. Mater. **313-316**, 1150 (2003).
[7] T. Pütterich *et al*. Plasma Phys. Control. Fusion **55**, 124036 (2013).
[8] C. Angioni *et al*. Phys. Plasmas **22**, 055902 (2015).
[9] F.J. Casson *et al*. Plasma Phys. Control. Fusion **57**, 014031 (2015).
[10] M. Sertoli *et al*. Nucl. Fusion **55**, 113029 (2015).
[11] C.Angioni *et al*. Nucl. Fusion **57**, 056015 (2017).
[12] C. Bourdelle *et al*. Plasma Phys. Control. Fusion **58**, 014036 (2016).
[13] J. Citrin *et al*, submitted to Plasma Phys. Control. Fusion.
[14] G. Cenacchi and A. Taroni. Rapporto ENEA RT/TIB/88/5 (1988).
[15] M. Romanelli *et al*. Plasma and Fusion Research **9**, 3403023 (2014).
[16] S. Breton *et al*, this conference.